Journal of Power Sources 218 (2012) 254–260

Contents lists available at SciVerse ScienceDirect

Journal of Power Sources

journal homepage: www.elsevier.com/locate/jpowsour

Oxygen surface exchange properties of $La_{0.6}Sr_{0.4}Co_{0.8}Fe_{0.2}O_{3-\delta}$ coated with $Sm_xCe_{1-x}O_{2-\delta}$

Tao Hong [a], Lei Zhang [a,b], Fanglin Chen [b], Changrong Xia [a,*]

[a] CAS Key Laboratory of Materials for Energy Conversion, Department of Materials Science and Engineering, University of Science and Technology of China, Hefei, Anhui 230026, China
[b] Department of Mechanical Engineering, University of South Carolina, Columbia, SC 29208, USA

HIGHLIGHTS

- Surface exchange coefficient has significantly increased for SDC coated LSCF.
- Surface exchange coefficient of SDC coated LSCF depends on the SDC loading.
- Exchange coefficient of SDC coated LSCF increases with ionic conductivity of SDC.

GRAPHICAL ABSTRACT

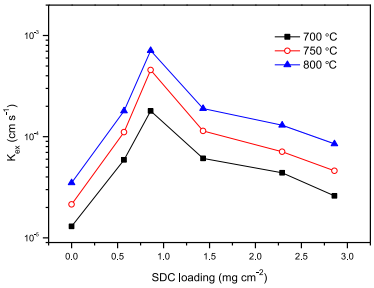

ARTICLE INFO

Article history:
Received 6 April 2012
Received in revised form
29 June 2012
Accepted 1 July 2012
Available online 7 July 2012

Keywords:
Surface exchange coefficient
Electrical conductivity relaxation
Lanthanum Strontium Cobaltite Ferrite
Doped ceria
Solid oxide fuel cells

ABSTRACT

Chemical oxygen surface exchange coefficient (K_{ex}) of $La_{0.6}Sr_{0.4}Co_{0.8}Fe_{0.2}O_{3-\delta}$ (LSCF) coated with samaria-doped ceria (SDC) particles has been investigated using the electrical conductivity relaxation method. It has been found that adding doped ceria to LSCF results in an increase of a factor of 10 in surface exchange rate, suggesting that oxygen incorporation at the LSCF/SDC/gas boundary sites is facile. Furthermore, K_{ex} of the SDC coated LSCF increases with the conductivity of SDC rather than the composition of the SDC, inferring that SDC supplies additional free oxygen vacancies for the surface exchange reaction. These results demonstrate that introducing doped ceria to $La_{1-x}Sr_xCo_{1-y}Fe_yO_{3-\delta}$ can substantially enhance the oxygen surface incorporation process for applications such as solid oxide fuel cell cathodes as well as oxygen separation membranes.

© 2012 Elsevier B.V. All rights reserved.

1. Introduction

$La_{1-x}Sr_xCo_{1-y}Fe_yO_{3-\delta}$ (LSCF) is a mixed ionic and electronic conductor that has attracted much attention as cathode material in solid oxide fuel cells (SOFCs) operating at intermediate temperatures. The relatively high ionic conductivity in LSCF extends the cathodic reaction zone beyond the electrode–electrolyte interface, resulting in high electrochemical performance compared with the classical strontium doped lanthanum manganite (LSM), which has negligible ionic conductivity. However, the performance of pure $La_{1-x}Sr_xCo_{1-y}Fe_yO_{3-\delta}$ electrode is still limited by the oxygen ion transport process within the electrode bulk in addition to the oxygen exchange process at the surface. For example, Adler et al. have experimentally and theoretically demonstrated that cathodic reaction of $La_{0.6}Sr_{0.4}Co_{0.2}Fe_{0.8}O_{3-\delta}$ on gadolinia-doped ceria is dominated by both the oxygen ion transport and oxygen surface exchange processes [1,2]. To enhance the transport process of the LSCF electrode, doped ceria is often introduced, which can substantially improve the electrochemical performance. By

* Corresponding author. Tel.: +86 551 3607475; fax: +86 551 3601592.
E-mail address: xiacr@ustc.edu.cn (C. Xia).

0378-7753/$ – see front matter © 2012 Elsevier B.V. All rights reserved.
http://dx.doi.org/10.1016/j.jpowsour.2012.07.004

adding 36 vol% $Gd_{0.1}Ce_{0.9}O_{2-\delta}$, Dusastre and Kilner have reduced four times the interfacial polarisation resistance of $La_{0.6}Sr_{0.4}Co_{0.2}Fe_{0.8}O_{3-\delta}$ electrode on $Gd_{0.1}Ce_{0.9}O_{2-\delta}$ electrolyte [3]. When 50 vol% $Gd_{0.2}Ce_{0.8}O_{2-\delta}$ is added, Murray et al. have found a factor of ~10 decrease in the polarisation resistance of $La_{0.6}Sr_{0.4}Co_{0.2}Fe_{0.8}O_{3-\delta}$ electrode [4]. Recently, doped ceria has been introduced in the LSCF cathode using sol–gel coating [5] and infiltrating [6] techniques. The cell resistances are also significantly reduced with relatively small amount of doped ceria coated in the LSCF electrode. The substantial enhancement in electrochemical performance is usually considered to be caused by the enhanced ionic conductivity through additional rapid oxygen ion conducting path of doped ceria. However, electrochemical impedance spectroscopy shows that adding doped ceria can not only accelerate the oxygen ion transport kinetics but also improve the surface exchange rate [2,6]. It has been experimentally demonstrated by Esquirol et al. that adding doped ceria to $La_{1-x}Sr_xCo_{1-y}Fe_yO_{3-\delta}$ can substantially improve the oxygen ion conductivity [7]. They reported that the oxygen diffusion coefficient of $La_{0.6}Sr_{0.4}Co_{0.2}Fe_{0.8}O_{3-\delta}$ was almost doubled when 30 wt% $Gd_{0.2}Ce_{0.8}O_{2-\delta}$ was introduced. Meanwhile, they found the surface exchange coefficient did not change by incorporation of doped ceria. This is in conflict with the impedance spectroscopic result in which the arc associated with the surface process was also reduced when doped ceria was added in the LSCF cathode. The conflict suggests that the effect of introducing doped ceria in LSCF electrode on the surface exchange process is still not well understood. This work aims to fill the knowledge gap and demonstrates that the oxygen surface exchange rate and the surface exchange coefficient of $La_{0.6}Sr_{0.4}Co_{0.8}Fe_{0.2}O_{3-\delta}$ are significantly increased with coating samaria-doped ceria particles. Accordingly, the improved cathode performance is due to the increased oxygen surface exchange coefficient in addition to the enhanced oxygen ionic conductivity when doped ceria is introduced to the LSCF electrode.

Measurement of oxygen surface exchange coefficients has typically been performed employing isotope exchange techniques with analysis of the exchanging gas phase or secondary ion mass spectrometry analysis of the exchanged ceramic samples. These methods are performed in thermodynamic equilibrium by keeping the oxygen partial pressure throughout the measurement, thus yielding the true coefficients. For mixed conductors such as $La_{1-x}Sr_xCo_{1-y}Fe_yO_{3-\delta}$, the coefficients can be determined with facile methods such as conductivity and weight relaxation methods [8,9]. These methods determine the chemical surface exchange coefficients by varying the oxygen partial pressure. In this work, the chemical coefficients are determined with the electrical conductivity relaxation method.

2. Experimental

$La_{0.6}Sr_{0.4}Co_{0.8}Fe_{0.2}O_{3-\delta}$ (LSCF) powders were synthesised using conventional solid state reaction method. La_2O_3, $SrCO_3$, Fe_2O_3 and Co_3O_4 (Sinopharm Chemical Reagent Co. Ltd) were used as the precursors and mixed at stoichiometric ratio by ball milling the components in ethanol for 24 h and calcined at 1000 °C for 5 h to form LSCF powders with single perovskite structure. The calcined powders were then ground, pressed into a rectangular bar at 300 MPa, and sintered at 1350 °C for 5 h in air to form dense LSCF samples. The size of the sintered bars had dimensions of 40.00 × 5.42 × 0.90 mm^3. And all sintered samples were confirmed to possess a density in excess of 95% theoretical density determined using the Archimedes method. Samaria-doped ceria, $Sm_xCe_{1-x}O_{2-\delta}$ (SDC) (x = 0.05, 0.1, 0.2, 0.3 and 0.4) powders were prepared using the carbonate co-precipitation method. Cerium and samarium nitrates ($Ce(NO_3)_3$, $Sm(NO_3)_3$, analytical grade, Sinopharm Chemical Reagent Co. Ltd) were used as the cation source, and ammonia carbonate ($(NH_4)_2CO_3$) was used as the precipitant. The cerium–samarium nitrate solution had a cation concentration of 0.1 mol L^{-1} with molar ratio of Sm^{3+}:Ce^{3+} = x:(1 − x). The nitrate solution was dropwise added into a 0.1 mol L^{-1} ammonium carbonate solution under mild stirring to form white carbonate precipitates at room temperature. The white precipitates were washed with distilled water three times and subsequently washed with ethanol. The washed precursor was dried at 70 °C for 48 h, and then calcined at 600 °C for 2 h to obtain SDC powders with single fluorite structures [10]. The SDC powders were mixed with ethanol and organic additives, and ball-milled for 48 h to obtain stable suspensions. The composition of the suspension was SDC:ethanol:organic additives = 1:10:0.5, in weight ratio. The LSCF bar samples were immersed into the SDC suspensions to coat SDC particles on LSCF surfaces. After coating, the samples were dried at room temperature and then heat-treated at 1000 °C for 2 h. The coating–drying–heating cycle was repeated to increase the SDC loading on the LSCF surface, which was determined by weighing the sample with electronic precision balance (METTLER TOLEDO AB135-S). The crystal structures of LSCF and SDC were identified using X-ray diffractometry (XRD, Philips X'pert PROS diffractometer). The microstructure was revealed using scanning electron microscopy (SEM, JSM-6700F). The porosity of the coated SDC layer was estimated with the SDC loading layer thickness.

The SDC powders were uniaxially dry-pressed under 300 MPa into pellets with 13 mm in diameter and sintered at 1400 °C for 5 h in air to obtain dense SDC samples for ionic conductivity measurement. The conductivity, σ, was measured in air by electrochemical impedance spectroscopy with an electrochemical workstation (ZHANER im6ex). Silver paste was applied to both sides of the sintered SDC samples and heated at 600 °C for 2 h to form the electrodes. The total d.c. conductivity of LSCF bars was measured by a standard, four-probe method using a measurement system insisting of a digital multimeter (Keithley 2001) interfaced with a computer and a program written using the LABVIEW 8.5 software. Silver wires were used as the lead wires, which were attached to the Ag electrode using silver paste followed by annealing in air at 600 °C for 2 h. The conductivity was measured at the temperatures of 700, 750 and 800 °C, respectively. For electrical conductivity relaxation measurement, LSCF bar samples were completely equilibrated at the atmosphere of Po_2 = 0.01 bar (O_2 + N_2) and then the oxygen partial pressure was abruptly changed to 0.1 bar (O_2 + N_2) while recording the electrical conductivity of the LSCF bar samples with time until a new equilibrium was reached [11]. The total gas flow rate was maintained at 300 ml min^{-1} to ensure that the Po_2 of the gas achieved equilibrium in no more than 20 s. The change in conductivity with time is plotted as $(\sigma(t) - \sigma(0))/(\sigma(\infty) - \sigma(0))$, where $\sigma(0)$, $\sigma(t)$ and $\sigma(\infty)$ denote the initial, time dependent and final conductivities, respectively. The experimental data is fitted to the theoretical equations as outlined by Lane and Kilner [12] for conductivity relaxation to derive the oxygen surface exchange and the oxygen diffusion coefficients.

3. Results and discussion

Fig. 1 shows the normalised conductivity for bare LSCF samples (LSCF samples without the SDC coating) at 700 °C when the oxygen partial pressure has been changed from 0.01 to 0.1 bar. The fitted curve is also shown. It can be seen that the experimental data matches very well with the fitting curve. The relaxation time is

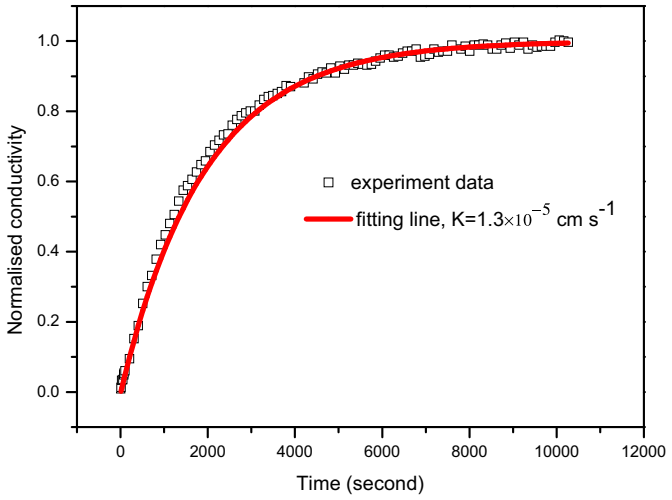

Fig. 1. Experimental data and fitting curve of conductivity change at 700 °C as a function of time.

about 10,000 s. The chemical oxygen diffusion coefficient, D_{chem}, is determined from the fitting result to be 6.4×10^{-6} cm^2 s^{-1} while the surface exchange coefficient, K_{ex}, is 1.3×10^{-5} cm s^{-1} at 700 °C. Bouwmeester et al. have previously investigated the oxygen transport in $La_{0.6}Sr_{0.4}Co_{0.8}Fe_{0.2}O_{3-\delta}$ using the electrical conductivity method by changing the oxygen partial pressure from 0.21 to 0.1 bar with samples in the size of $25 \times 15 \times 0.53$ mm^3 [13]. Their results show that K_{ex} at 700 °C is about 1×10^{-5} cm s^{-1}, which agrees well with the present result. Katsuki et al. have measured the oxygen transport properties using the weight relaxation method through thermogravimetric measurement [14]. Their results are $D_{chem} = 5 \times 10^{-6}$ cm^2 s^{-1} and $K_{ex} = 0.7 \times 10^{-5}$ cm s^{-1} at 700 °C for $La_{0.6}Sr_{0.4}Co_{0.8}Fe_{0.2}O_{3-\delta}$ when the oxygen partial pressure is changed from 0.37 to 0.5 bar. Both D_{chem} and K_{ex} are similar to the present results. It should be noted that the chemical surface exchange coefficient, on which the present work is focused, is consistent to those reported, indicating that the electrical conductivity relaxation method employed in this study is a reliable technique to study the surface exchange coefficient for LSCF coated with SDC particles.

Fig. 2 presents the electrical conductivity relaxation profiles at 750 °C for LSCF samples coated with different amount of $Sm_{0.2}Ce_{0.8}O_{1.9}$. When LSCF is not coated with SDC, the relaxation time is about 7800 s. It decreases to 2000 s when 0.57 mg cm^{-2} SDC is coated, and further to 1200 s at SDC loading of 0.86 mg cm^{-2}. However, when the SDC loading is further increased, the relaxation time increases: it is 2000 s when the SDC loading is 1.43 mg cm^{-2} and 4500 s when the SDC loading reaches 2.86 mg cm^{-2}. The ionic transport properties within LSCF bulk should not be affected by the surface properties, i.e., the deposited SDC on LSCF surface would not be expected to change D_{chem}. Therefore, the change in relaxation time with different SDC loading seems to be due to the variation on surface exchange rate of SDC coated LSCF since the gas phase conditions are kept the same. Low relaxation time means high surface exchange rate. The surface exchange on LSCF proceeds in the fastest way when 0.86 mg cm^{-2} SDC particles are introduced. Its relaxation time is only 1/6 of bare LSCF, i.e., LSCF with no SDC coating, indicating substantial improvement in surface exchange rate when SDC particles are coated on LSCF surface. Since D_{chem} is the same for all the samples, the enhanced exchange kinetics must be attributed to K_{ex}. In this case, K_{ex} can be easily derived with one-parameter fitting process using constant D_{chem} at a given temperature. Fig. 3 shows K_{ex} values at 700, 750 and 800 °C for different SDC loading. It can be seen that K_{ex} values of the SDC coated LSCF samples are larger than that of the bare LSCF. In addition, K_{ex} is affected by the SDC loading. When the loading is 0.86 mg cm^{-2}, K_{ex} reaches the largest value of 4.57×10^{-4} cm s^{-1} at 750 °C, which is more than one order of magnitude higher than that of bare LSCF, 2.7×10^{-5} cm s^{-1}. However, when the SDC loading is further increased, K_{ex} decreases. It is 4.6×10^{-5} cm s^{-1} at 2.86 mg cm^{-2}.

Fig. 4a and b shows the surface and cross-section of bare LSCF bar sample. It is clear that the bars are completely dense. The grains' size varies between 5 and 30 μm and there are only several isolated holes which are less than 2 μm in the cross-section. Fig. 4c and d presents the bars coated with 0.57 and 0.86 mg cm^{-2} SDC particles, which increases K_{ex} from 2.7×10^{-5} to 1.11×10^{-4} and 4.57×10^{-4} cm s^{-1} at 750 °C, respectively. Fig. 4e and f is the surface microstructure of LSCF bars coated with 1.43 and 2.86 mg cm^{-2} SDC particles. It is obvious that more LSCF surface is

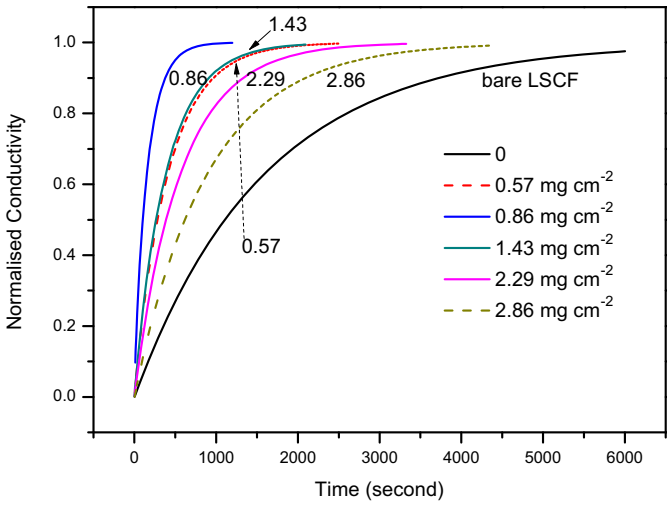

Fig. 2. Relaxation curves at 750 °C for LSCF bars coated with different amount of $Sm_{0.2}Ce_{0.8}O_{1.9}$ particles.

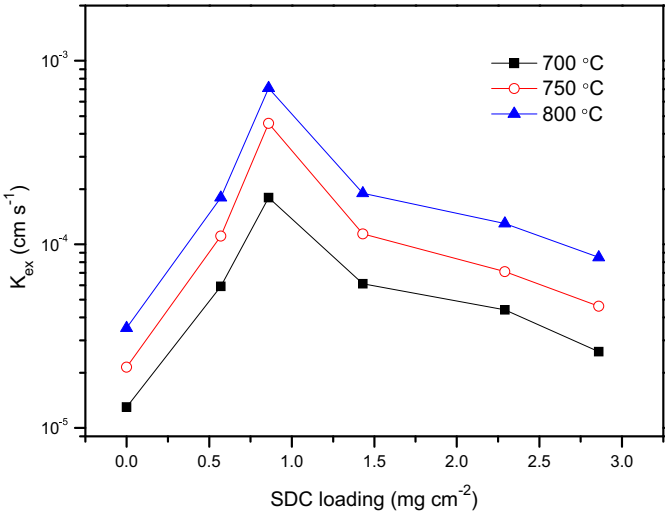

Fig. 3. Oxygen surface exchange coefficient, K_{ex}, for LSCF bars coated with different amount of $Sm_{0.2}Ce_{0.8}O_{1.9}$.

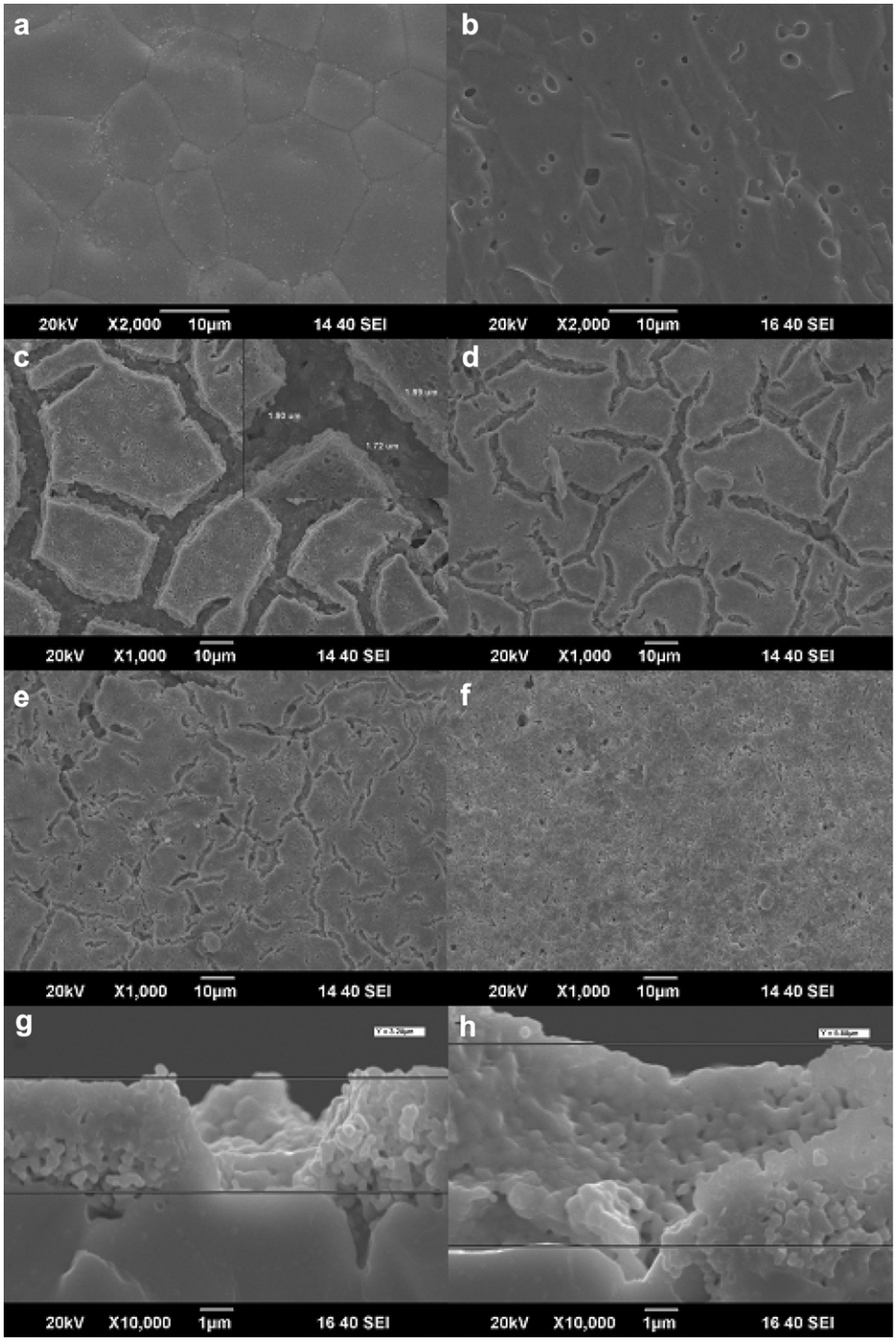

Fig. 4. SEM micrographs, (a) Bare LSCF surface, (b) Cross-section of LSCF bar, surface coated with (c) 0.57 mg cm^{-2}, (d) 0.86 mg cm^{-2}, (e) 1.43 mg cm^{-2}, and (f) 2.86 mg cm^{-2} SDC particles, SDC–LSCF interface with (g) 2.29 mg cm^{-2}, and (h) 2.86 mg cm^{-2} SDC particles.

covered as the SDC loading is increased. When 2.86 mg cm^{-2} SDC is deposited, LSCF surface can not be seen from the SEM picture.

It could be seen that oxygen exchange at bare LSCF occurs only at the LSCF/gas interface, the exchange at the coated sample could happen at three different sites: the LSCF/gas interface, the SDC/gas interface, and the LSCF/SDC/gas three-phase boundary. It has been demonstrated that the surface exchange coefficient of doped ceria is much lower than that of LSCF [12,15]. So, SDC/gas interface is not the reason for the enhanced exchanging kinetics. The SDC particles cover most of the LSCF surface, which suggests that the amount of oxygen exchanged at the LSCF/gas interface should be reduced as a result of SDC coating. Accordingly, the enhanced exchange kinetics must be caused by the three-phase boundary. The coated SDC particles do not form a dense layer on LSCF but leave many cracks for gas phase transportation. At the cracks, the gas phase/SDC/LSCF confront together to form the three-phase boundary,

where oxygen incorporation reactions could be enhanced. The boundary is constructed once SDC is coated and its length increases with SDC loading. However, when the coating–heating cycle is repeated, the cracks are gradually filled with SDC particles, Fig. 4e and f. The filling blocks the gas transportation, thus decreases the effective three-phase boundary length, and consequently reduces the exchange rate as shown in Fig. 3. Fig. 4g and h shows the SDC–LSCF interface micrographs for LSCF bars coated with 2.29 and 2.86 mg cm^{-2} SDC, respectively. The thickness of the coating could be determined with the SEM analysis. The porosity is estimated with the loading, thickness, and density of SDC. The thickness of the coated layer is about 1.9 μm at the loading of 0.57 mg cm^{-2}, corresponding to a porosity of about 66%. When the loading reaches 2.86 mg cm^{-2}, the thickness increases to 5.8 μm and the porosity decreased to 35%.

Fig. 5 shows the Arrhenius plots of K_{ex}. The activation energy for bare LSCF is 86.4 kJ mol^{-1}, which is close to that for $La_{0.6}Sr_{0.4}Co_{0.2}Fe_{0.8}O_{3-\delta}$, 105 ± 14 kJ mol^{-1} [16], and quite lower than that reported for $La_{0.6}Sr_{0.4}Co_{0.8}Fe_{0.2}O_{3-\delta}$, about 190 kJ mol^{-1} obtained with weight relaxation method [14]. It is noted that, when LSCF is coated with SDC, the activation energy increases but is still close to that for bare LSCF, suggesting that the surface exchange mechanism for LSCF is not significantly affected by SDC coating.

The kinetics of the oxygen exchange reaction may be coupled to molecular diffusion and surface transport processes, as well as to bulk ionic and electronic transport [17]. In our experiment, the driving force condition is kept the same and the bulk transport properties are identical. Therefore, the variation in oxygen surface exchange kinetics for LSCF is likely to be due to the surface conditions. For LSCF surface coated with SDC, oxygen exchange can occur at any of the following sites exposed to the gas phase: i) on the LSCF surface, ii) on the SDC surface, and iii) on the LSCF/SDC interface. Comparing to LSCF with no SDC coating, coating SDC to LSCF increases the surface exchange rate, i.e., reduces the relaxation time. The increase in surface exchange rate for LSCF coated with SDC is unlikely to be attributed to the surface exchange reaction on the SDC surface because LSCF is much more active to oxygen exchange compared to that of doped ceria [18]. In addition, the activation energy of the surface exchange of LSCF coated with SDC is almost not changed by SDC addition, as shown in Fig. 5. On the other hand, the increase in surface exchange rate for LSCF coated with SDC can neither be attributed to the LSCF surface since the effective surface area exposed to the gas phase should have been reduced when SDC is deposited on LSCF surface. Therefore, the increase in surface exchange rate for LSCF coated with SDC may be originated from the reaction occurring at the LSCF/SDC interface where gas is available. In addition, the increase in surface exchange rate for LSCF coated with SDC indicates that the oxygen exchange process across the LSCF/SDC interface is facile, i.e., the oxygen exchange process occurs mainly at the LSCF/SDC/gas three-phase boundary (TPB) sites. The exchange rate at TPB must be substantially higher than that on LSCF surface. Once SDC is coated on LSCF, the LSCF/SDC interface is generated, resulting in an increase of the surface exchange rate although SDC particles reduce the effective LSCF surface area for oxygen exchange. The amount of TPB depends on the SDC loading on the LSCF surface. When the SDC loading is too low, only very limited LSCF/SDC interface is generated. On the other hand, when the SDC loading is too high, the effective LSCF/SDC/gas boundary length is also low since gas phase is not available due to high SDC coverage. In this work, when 0.86 mg cm^{-2} SDC is coated on LSCF surface, the effective TPB should be the largest since the sample exhibits the highest exchange rate and the largest K_{ex}.

Fig. 6 shows the conductivity relaxation profiles at 750 °C for bare LSCF samples as well as LSCF samples coated with $Sm_xCe_{1-x}O_{2-\delta}$ in which $x = 0.05–0.4$. The SDC loading is almost the same for every SDC coated sample, about 1.43 mg cm^{-2}. The relaxation time, tr, is also shown in Fig. 6 in order to compare the oxygen surface exchange rates. It can be clearly seen that the conductivity relaxation time which depends on SDC composition, i.e., x in $Sm_xCe_{1-x}O_{2-\delta}$, decreases significantly for all the SDC coated samples and reaches the lowest value of 2000 s when $x = 0.2$. The tr–x relationship suggests that the oxygen surface exchange rate as well as its coefficient depend on the samarium content in SDC. Fig. 7 shows K_{ex} values at 700, 750 and 800 °C versus SDC composition and clearly illustrates that K_{ex} is affected by the SDC composition. K_{ex} reaches its highest value at $x = 0.2$, which is 1.14×10^{-4} cm s^{-1} at 750 °C.

As shown in Fig. 7, surface exchange rate of LSCF coated with SDC is affected by SDC composition. Since the SDC composition also affects the ionic conductivity of doped ceria [19], it is reasonable to expect that the surface exchange coefficient might be related to the conductivity of SDC. Fig. 8 shows the conductivity at 700–800 °C of $Sm_xCe_{1-x}O_{2-\delta}$, which are prepared with

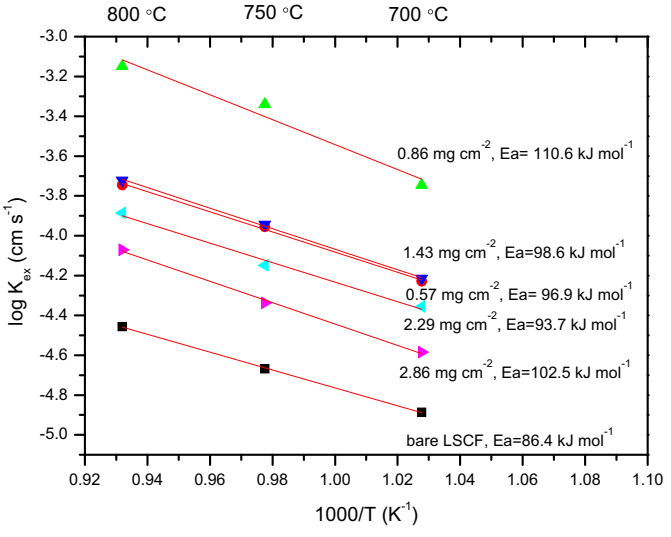

Fig. 5. Arrhenius plots of the oxygen surface exchange coefficients of LSCF coated with various amount of $Sm_{0.2}Ce_{0.8}O_{1.9}$.

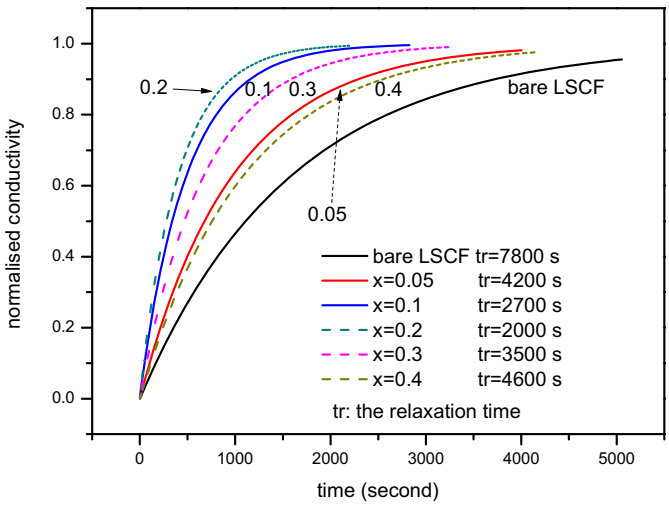

Fig. 6. Conductivity relaxation fitting curves at 750 °C for LSCF coated with $Sm_xCe_{1-x}O_{2-\delta}$.

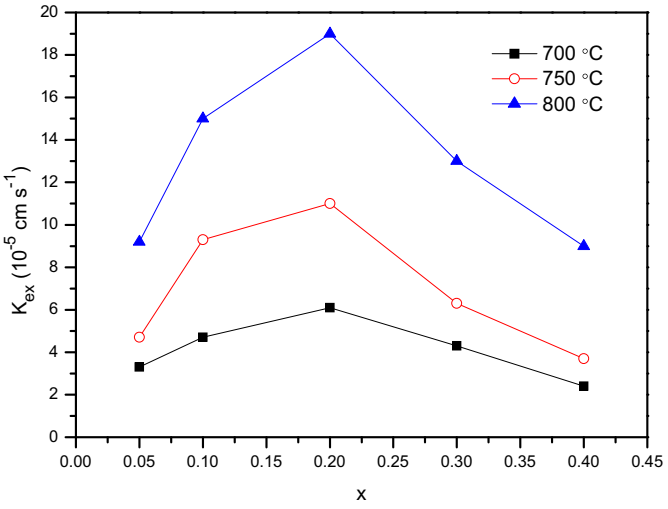

Fig. 7. Oxygen surface exchange coefficient K_{ex} for LSCF coated with $Sm_xCe_{1-x}O_{2-\delta}$ at different x values.

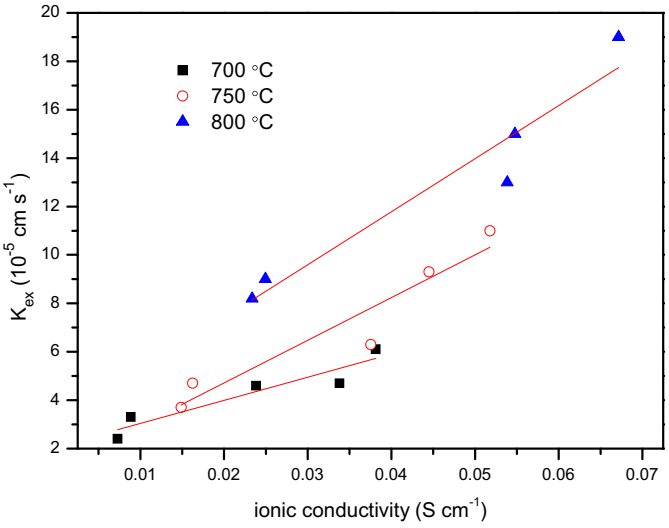

Fig. 9. Oxygen surface exchange coefficient K_{ex} versus SDC conductivity.

the same powders for coating on LSCF samples. SDC shows the highest conductivity at $x = 0.2$. The σ–x relationship is consistent with the previous report [19]. Comparing Fig. 8 with Fig. 7, it can be clearly seen that K_{ex} and σ have the similar dependence on x, suggesting that K_{ex} increases with σ. Fig. 9 presents the K_{ex}–σ curves at 700, 750 and 800 °C, respectively. K_{ex} increases almost linearly with σ, demonstrating that it is the conductivity of SDC rather than the composition of SDC that determines the surface exchange coefficients of SDC coated LSCF. For example, $Sm_{0.05}Ce_{0.95}O_{2-\delta}$ and $Sm_{0.4}Ce_{0.6}O_{2-\delta}$ have similar conductivity at 700, 750 and 800 °C. Although their compositions are quite different, the corresponding surface exchange coefficients are very close to each other.

The electrical conductivity relaxation experiment is conducted in oxygen partial pressure change from 0.01 to 0.1 bar. In this process, oxygen is incorporated to LSCF. The incorporation of oxygen from a gas phase into the bulk of a solid phase can be represented in Kroger–Vink notation by the following equations [18]:

$$\text{Adsorption}: \quad O_2(g) + S_{ads} \rightarrow (O_2)_{ads} \tag{1}$$

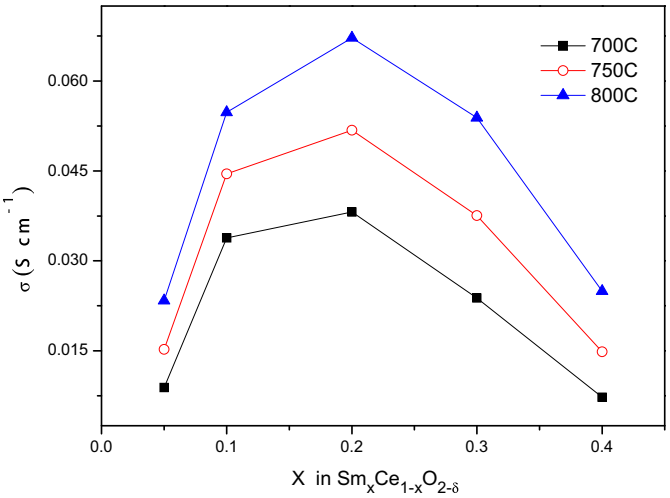

Fig. 8. Conductivity of $Sm_xCe_{1-x}O_{2-\delta}$ measured in air.

$$\text{Dissociation}: \quad (O_2)_{ads} + 4e^- \rightarrow 2O^{2-}_{ads} \tag{2}$$

$$\text{Incorporation}: \quad O^{2-}_{ads} + V_O^{\bullet\bullet} \rightarrow O_O^{\times} \tag{3}$$

and

$$\text{Overall reaction}: \quad O_2(g) + 4e^- + 2V_O^{\bullet\bullet} \rightarrow 2O_O^{\times} \tag{4}$$

where S_{ads} denotes the site for adsorption of oxygen on the solid surface. These equations show that oxygen incorporation involves sites for adsorption, available electrons and oxygen vacancies. For perovskite-type materials such as LSCF, the electronic conductivity is at least two orders of magnitude higher than the ionic conductivity and electrons enter as an energy shift through the Fermi level. Therefore, it can be assumed that electrons are sufficient in the step of dissociation and thus the charge-transfer may be a fast and energy free process [17]. Because of its relatively low ionic conductivity, few free oxygen vacancies are available and thus the incorporation step may limit the overall oxygen exchange process on LSCF. At the LSCF/SDC interface, this incorporation step might be enhanced due to the additional free oxygen vacancies supplied by SDC. The concentration of free oxygen vacancies is closely related to oxygen ionic conductivity [20]. Usually, the conductivity is proportional to the free oxygen vacancy concentration. Consequently, the surface exchange rate increases with SDC conductivity as shown in Fig. 9. It should be noted that, the total oxygen vacancy concentration of $Sm_{0.4}Ce_{0.6}O_{2-\delta}$ is much higher than that of $Sm_{0.05}Ce_{0.95}O_{2-\delta}$. However, too many oxygen vacancies in a solid can result in high defect association and eventually low free oxygen vacancy concentration. The free oxygen vacancy concentrations of $Sm_{0.4}Ce_{0.6}O_{2-\delta}$ and $Sm_{0.05}Ce0_{.95}O_{2-\delta}$ could be very close since their conductivities are similar.

It has been reported that adding LSCF particles on doped ceria surface leads to a 100-fold increase in surface exchange coefficients [18]. It is possible that LSCF provides electrons for the incorporation reaction on doped ceria. This work demonstrates that SDC particles on LSCF surface can dramatically increase the surface exchange rate of LSCF by providing additional free oxygen vacancies at the LSCF/SDC/gas boundary. Therefore, there might be synergistic action of doped ceria and LSCF for oxygen incorporation. Similar effects have also been observed on $La_{0.8}Sr_{0.2}MnO_3$ and $Sr_2Fe_{1.5}Mo_{0.5}O_6$ perovskites [21,22]. Such synergistic action is important in developing

solid state ionic devices such as cathodes for SOFCs and oxygen separation membranes.

4. Conclusion

Coating $Sm_xCe_{1-x}O_{2-\delta}$ particles on LSCF surface can substantially improve the oxygen surface exchange rate as well as the chemical oxygen surface exchange coefficient. When 0.86 mg cm^{-2} $Sm_{0.2}Ce_{0.8}O_{2-\delta}$ particles are coated on LSCF, the oxygen exchange coefficient increases from 2.7×10^{-5} for bare LSCF to 4.57×10^{-4} cm s^{-1} at 750 °C. The improvement in oxygen surface exchange kinetics depends on the amount of coated SDC particles, indicating facile oxygen incorporation reaction at the LSCF/SDC/gas boundary sites. The surface exchange coefficient increases almost linearly with ionic conductivity of $Sm_xCe_{1-x}O_{2-\delta}$, demonstrating that additional free oxygen vacancies are critical for oxygen incorporation in LSCF. The enhancement in surface exchange kinetics exhibits that introducing doped ceria to $La_{1-x}Sr_xCo_{1-y}Fe_yO_{3-\delta}$ can substantially facilitate the surface exchange process. Therefore, adding doped ceria to LSCF can improve the performance of electrochemical devices such as solid oxide fuel cells and oxygen separation membranes.

Acknowledgement

We gratefully acknowledge the financial support of the Ministry of Science and Technology of China (2012CB215403) and the US National Science Foundation (CBET 0967166).

References

[1] S. Adler, J.A. Lane, B.C.H. Steele, J. Electrochem. Soc. 143 (1996) 3554–3564.
[2] S. Adler, Chem. Rev. 104 (2004) 4791–4843.
[3] V. Dusastre, J.A. Kilner, Solid State Ionics 126 (1999) 163–174.
[4] E.P. Murray, M.J. Sever, S.A. Barnett, Solid State Ionics 148 (2002) 27–34.
[5] J.W. Yun, J. Han, S.P. Yoon, S. Park, H.S. Kim, S.W. Nam, J. Ind. Eng. Chem. 17 (2011) 439–444.
[6] J. Chen, F.L. Liang, B. Chi, J. Pu, S.P. Jiang, L. Jian, J. Power Sourc. 194 (2009) 275–280.
[7] A. Esquirol, J. Kilner, N. Brandon, Solid State Ionics 175 (2004) 63–67.
[8] J.E. Elshof, M.H.R. Lankhorst, H.J.M. Bouwmeester, Solid State Ionics 99 (1997) 15–22.
[9] I. Yasuda, M. Hishinuma, J. Solid State Chem. 123 (1996) 382–390.
[10] D. Ding, B.B. Liu, Z.N. Zhu, S. Zhou, C.R. Xia, Solid State Ionics 179 (2008) 896–899.
[11] J.E. ten Elshof, M.H.R. Lankhorst, H.J.M. Bouwmeester, J. Electrochem. Soc. 144 (1997) 1060–1067.
[12] J.A. Lane, J.A. Kilner, Solid State Ionics 136–137 (2000) 997–1001.
[13] H.J.M. Bouwmeester, M.W. Otter, B.A. Boukamp, J. Solid State Electrochem. 8 (2004) 599–605.
[14] M. Katsuki, S.R. Wang, M. Dokiya, T. Hashimoto, Solid State Ionics 156 (2003) 453–461.
[15] P.S. Manning, J.D. Sirman, J.A. Kilner, Solid State Ionics 93 (1997) 125–132.
[16] S.J. Benson, R.J. Chater, J.A. Kilner, in: T.A. Ramanarayanan (Ed.), Proceedings of the 3rd International Symposium on Ionic and Mixed Conducting Ceramics, Electrochemical Society Proceedings, vol. 97–24, 1998, p. 596. Pennington, New Jersey.
[17] S.B. Adler, X.Y. Chen, J.R. Wilson, J. Catal. 245 (2007) 91–109.
[18] J.D. Sirman, J.A. Kilner, J. Electrochem. Soc. 143 (1996) L229–L231.
[19] S.W. Zha, C.R. Xia, G.Y. Meng, J. Power Sourc. 115 (2003) 44–48.
[20] H. Yahiro, Y. Eguchi, K. Eguchi, H. Arai, J. Appl. Electrochem. 18 (1988) 527–531.
[21] Y. Wang, L. Zhang, C.R. Xia, Int. J. Hydrogen Energy 37 (2012) 2182–2186.
[22] L. Zhang, Y.Q. Liu, Y.X. Zhang, G.L. Xiao, F.L. Chen, C.R. Xia, Electrochem. Commun. 13 (2011) 711–713.